Journal of Astronomical Telescopes, Instruments, and Systems

AstronomicalTelescopes.SPIEDigitalLibrary.org

Wide field imager instrument for the Advanced Telescope for High Energy Astrophysics

Norbert Meidinger
Kirpal Nandra
Markus Plattner
Matteo Porro
Arne Rau
Andrea Santangelo
Chris Tenzer
Jörn Wilms

SPIE.

Wide field imager instrument for the Advanced Telescope for High Energy Astrophysics

Norbert Meidinger,[a,*] Kirpal Nandra,[a] Markus Plattner,[a] Matteo Porro,[a] Arne Rau,[a] Andrea Santangelo,[b] Chris Tenzer,[b] and Jörn Wilms[c]
[a]Max-Planck-Institut für Extraterrestrische Physik, Giessenbachstrasse, Garching D-85748, Germany
[b]Univ. Tübingen, Institut für Astronomie und Astrophysik, Sand 1, Tübingen D-72076, Germany
[c]Univ. Erlangen-Nürnberg, Dr. Karl Remeis-Sternwarte, Sternwartstrasse 7, Bamberg D-96049, Germany

Abstract. The Advanced Telescope for High Energy Astrophysics (Athena) has been selected for ESA's L2 mission, scheduled for launch in 2028. It will provide the necessary capabilities to achieve the ambitious goals of the science theme "The Hot and Energetic Universe." Athena's x-ray mirrors will be based on silicon pore optics technology with a 12-m focal length. Two complementary focal plane camera systems are foreseen, which can be moved interchangeably to the focus of the mirror system: the actively shielded micro-calorimeter spectrometer X-IFU and the wide field imager (WFI). The WFI camera will provide an unprecedented survey power through its large field of view of 40 arc min with a high count-rate capability (~1 Crab). It permits a state-of-the-art energy resolution in the energy band of 0.1 to 15 keV during the entire mission lifetime (e.g., full width at half maximum ≤150 eV at 6 keV). This performance is accomplished by a set of depleted P-channel field effect transistor (DEPFET) active pixel sensor matrices with a pixel size well suited to the angular resolution of 5 arc sec (on-axis) of the mirror system. Each DEPFET pixel is a combined detector-amplifier structure with a MOSFET integrated onto a fully depleted 450-μm-thick silicon bulk. This manuscript will summarize the current instrument concept and design, the status of the technology development, and the envisaged baseline performance. © *The Authors. Published by SPIE under a Creative Commons Attribution 3.0 Unported License. Distribution or reproduction of this work in whole or in part requires full attribution of the original publication, including its DOI.* [DOI: 10.1117/1.JATIS.1.1.014006]

Keywords: camera; detector; imaging; silicon; spectroscopy; x-ray.

Paper 14021P received Aug. 20, 2014; accepted for publication Nov. 21, 2014; published online Dec. 30, 2014.

1 Introduction

The Advanced Telescope for High Energy Astrophysics (Athena) will be the next large-class x-ray observatory of the European Space Agency (ESA) with a launch anticipated for 2028.[1] It is designed to answer two of the most pressing questions in astrophysics about the assembly of ordinary matter into large scale structures and the growth and evolution of black holes. Athena's science theme "The Hot and Energetic Universe" was endorsed by ESA in late 2013, and the Athena mission proposal was accepted by ESA in June 2014.

The Athena telescope concept comprises a single large-aperture x-ray telescope based on silicon pore optics technology.[2] The mirror system will provide effective areas of 2 and 0.25 m^2 at energies of 1 and 6 keV, respectively. It will image the x-ray photons onto one of two complementary and interchangeable focal plane instruments: the x-ray integral field unit (X-IFU) and the wide field imager (WFI). The X-IFU provides very high spectral resolution over a small field of view by using transition edge sensors operated at cryogenic temperatures.[3] The WFI offers good spectral resolution over a broad energy band (0.1 to 15 keV) and a very large field of view of 40 arc min coupled with a very fast readout.[4] The WFI capabilities are needed to map large areas of the x-ray sky to great depths, required, for example, to reveal typical black holes growing in the early universe at $z > 6$ and to track their growth and influence on the wider universe through cosmic time.

The design of the WFI instrument will be presented in the next section. A brief introduction of the key element, the depleted P-channel field effect transistor (DEPFET) detector and its necessary further development are given in Sec. 3. Control and data acquisition electronics as well as further subsystems of the WFI camera are described in Secs. 4 and 5, respectively. The tentative schedule for the instrument development concludes the description of the WFI camera for the Athena project.

2 Conceptual Instrument Design

The WFI will comprise the following subsystems (see Fig. 1), which are mounted to the primary structure of the instrument that provides the necessary stability:

Camera head with detector array: Each of the five DEPFET sensors forms together with the front-end ASICs, both integrated in the associated detector board, a separate and modular unit. The detector array is surrounded by a graded Z-shield (Z = atomic number of the used material) to minimize the instrument background and a proton shield to reduce radiation damage, i.e., to ensure long-term stability of the detector performance. The graded Z-shield absorbs fluorescence photons generated in one layer in the proximate inner layer with lower atomic number Z. This is a similar approach as designed for the camera system of the eROSITA instrument onboard the SRG mission.[5,6] Mitigation of radiation damage is accomplished by cooling of the detectors. For this purpose, they are linked via heat pipes to a

*Address all correspondence to: Norbert Meidinger, E-mail: meidinger@mpe.mpg.de

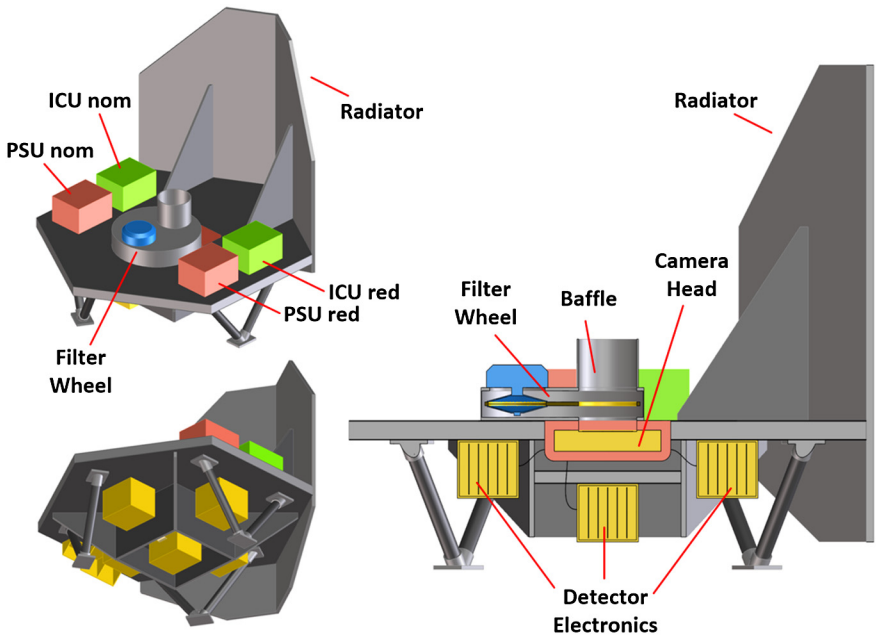

Fig. 1 Schematic view of the WFI instrument with the camera head comprising the five depleted P-channel field effect transistor (DEPFET) detectors, the dedicated detector electronics arranged in five boxes, the filter wheel in front of the camera, the power supply unit (nominal and redundant), and the instrument control unit (nominal and redundant). For a movement of the camera into the focus of the mirror system, the radiators have to be moved as well. The alternative is to tilt the mirror system and leave the cameras in fixed positions.

radiator. A nominal operating temperature of −60°C or lower is aimed for and needs control, e.g., by heaters, to be kept stable.

Detector electronics: The five detectors are connected with flexible leads to their dedicated electronics. Detector electronics boxes are mounted underneath the camera platform.

Filter wheel: The filter wheel is mounted in front of the detector and will provide at least the following options:

1. a light-blocking filter.
2. an on-board calibration source.
3. an open position for evacuation or observations without filter.
4. a closed position for shielding and sensor protection.

The aperture of the filter wheel is equipped with a stray light baffle.

Power supply unit (PSU): The power for the WFI instrument is supplied by the spacecraft to the PSU that controls and distributes it to the subsystems. The PSU will be a redundant system, with nominal and redundant units, to minimize the risk of instrument breakdown.

Instrument control unit: The instrument control unit (ICU) provides the communication interface between the spacecraft and the instrument. Due to these important functions, the ICU shall also be designed with nominal and redundant units.

An overview of the subsystem functionalities is shown in Fig. 2. The ICU and the power supply unit act as electronic interfaces to the spacecraft. Both are connected to the five detector electronics for power supply, detector control, and data transfer. The detector electronics in turn supply and control the camera head and receive in return the analog output signals of the detectors. Attached to the camera head is the filter wheel, which controls the photon flux from the mirror system to the DEPFET sensors. The sensors are electrically connected to the control and analog front-end electronics (CFE and AFE) that are part of the camera head and thermally linked to the radiator for cooling.

2.1 *Focal Plane Design*

Due to its physical size of ∼14 cm, the focal plane detector cannot be realized as a single monolithic device. Instead, it will be composed of a combination of four large DEPFET arrays designed to cover the large field of view and one smaller DEPFET optimized for fast timing applications (see Sec. 3.3). Several options for the location of the fast detector are currently being studied. Placing it in the center, as shown in Fig. 3, has the advantage of compactness and permits the observation of very bright sources simultaneously with objects in the large field of view. However, this option requires detailed analysis because of two issues: the complexity in arranging the front-end electronics behind the sensor (i.e., the far side with respect to the mirror system) and as a consequence, the impairment of the graded Z-shield.

An alternative solution could be to accommodate the fast sensor adjacent on the four large sensors. Depending on whether the observation requires a large field of view for large objects or a small detector with high-time resolution for very bright point sources, the respective detector will be moved in the focal plane to the on-axis position of the mirror system. This arrangement is beneficial for the placement of the front-end electronics including thermal and mechanical interfaces, for the modularity of the focal plane detector and for the implementation of the graded Z-shield.

For a sufficient oversampling of the on-axis PSF of 5 arc sec half energy width of the mirror system, the pixel size has to be matched. With a pixel size of $100 \times 100\ \mu m^2$, the PSF is oversampled by a factor of 2.8. Actually, the oversampling is almost a factor of two higher since the signal charge of an x-ray photon is spread over up to four pixels allowing a more accurate spatial resolution.

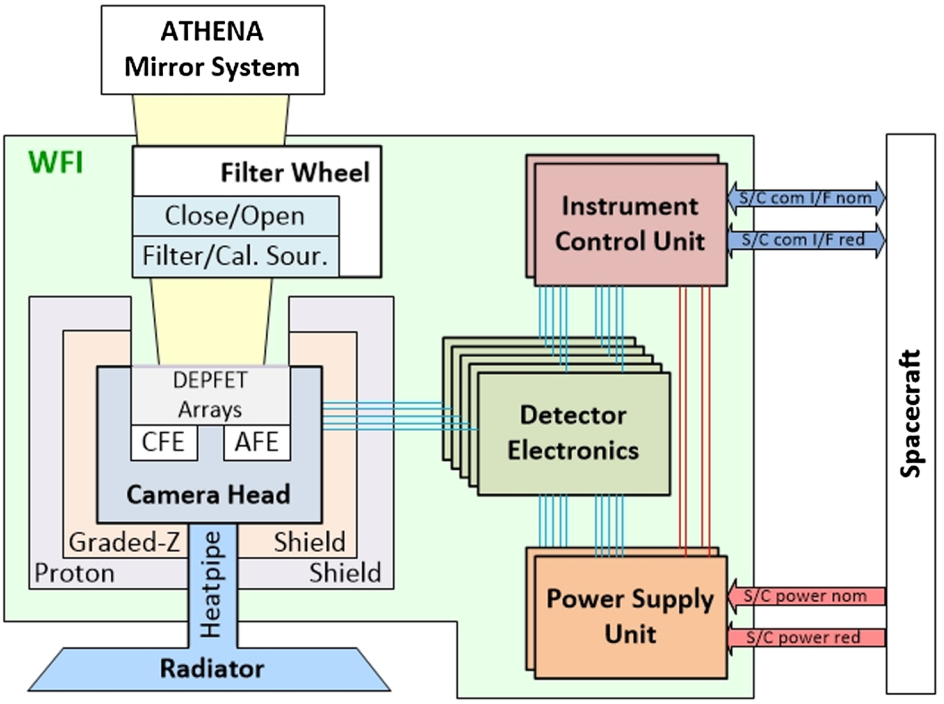

Fig. 2 Block diagram of the WFI instrument with subsystems and interfaces.

3 DEPFET Detector

Each of the five detectors has the following main components: the DEPFET active pixel sensor (APS), the readout ASICs of VERITAS-2 type, the switcher control ASICs, and a detector board with integrated electrical interface to the detector electronics that is located outside the focal plane. DEPFET detectors have been developed as prototypes for previous x-ray astronomy mission proposals, e.g., IXO, and as flight detectors for the MIXS instrument on-board of ESA's BepiColombo satellite to Mercury.[7]

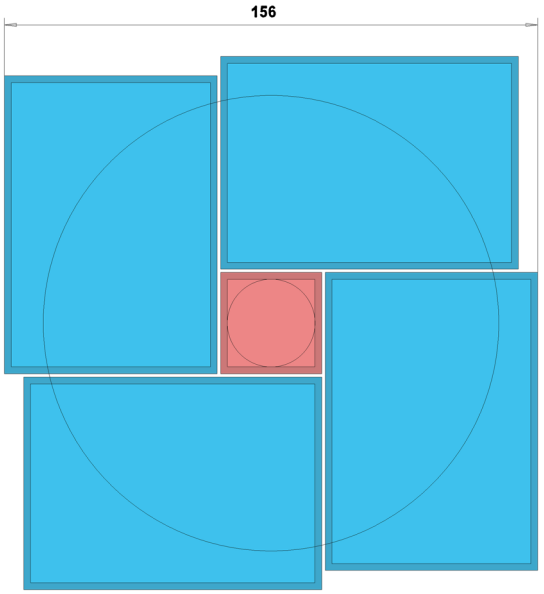

Fig. 3 Potential layout of the five focal plane detectors for the WFI: a small but fast DEPFET detector in the center for bright sources (approximately 7 arcmin) and four identical, large-area DEPFET detectors surrounding the central one to span the large field of view of 40 arcmin (indicated as outer circle).

3.1 *DEPFET APS Concept*

The APS planned for the WFI instrument use DEPFETs as signal amplifying element per pixel (Fig. 4). The signal electrons generated by the interaction of an incident x-ray photon with the fully (sideways) depleted silicon bulk are collected in an internal gate underneath the transistor channel. This increases the conductivity of the MOSFET proportional to the number of stored signal electrons and is, therefore, a measure of the energy of the incident photon. The internal gate persists regardless of the presence of a transistor current. Thus, the pixels are switched on for readout only and are switched off during the remaining time until the next readout occurs. The amount of integrated charge can then be sensed by turning on the transistor current and measuring the difference of the conductivity before and after the charge removal as depicted in Fig. 5.

The pixels are organized in matrices with one global contact for the backside. The time-dependent control voltages for switching on the transistor currents and clearing of the signal charges in the internal gates are applied row-wise, whereas the signal readout is accomplished column-wise. A 64-channel fast and low-noise analog signal processor, called VERITAS-2, will serve for this purpose. This ASIC reads 64 pixels of a row in parallel (i.e., simultaneously) and multiplexes at the same time the signals of the previous row to one output buffer. The number of VERITAS-2 ASICs is chosen according to the number of pixels per row. The readout scheme is the following: one row is switched active and read out while the others are switched off but collect the signal charge generated by incoming x-ray photons. Next, the neighboring row is switched on for readout. This rolling shutter mode is continued until all pixels of the sensor are read out and the cycle starts again with the first row.

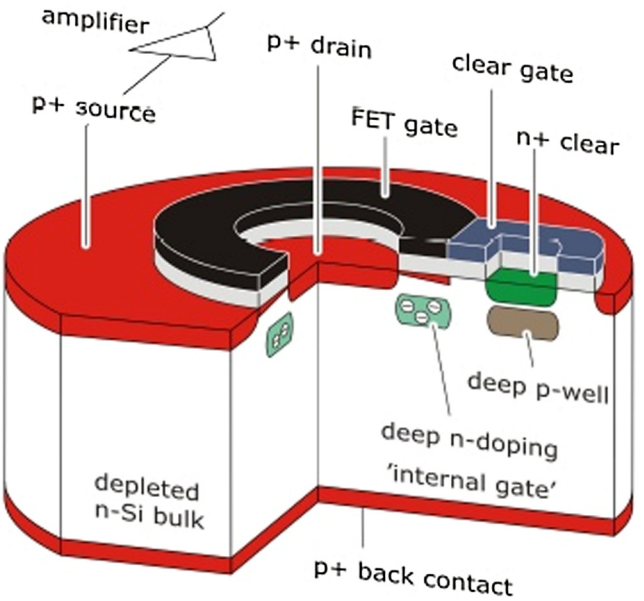

Fig. 4 Schematic view of a basic circular DEPFET transistor, which is the readout element of each pixel. The signal charge generated by an x-ray photon is collected and stored in the internal gate of the DEPFET located underneath the external gate deep in the pixel bulk volume. The transistor current increases for each electron in the internal gate by a certain amount, e.g., 0.3 nA, depending on the design of the DEPFET.

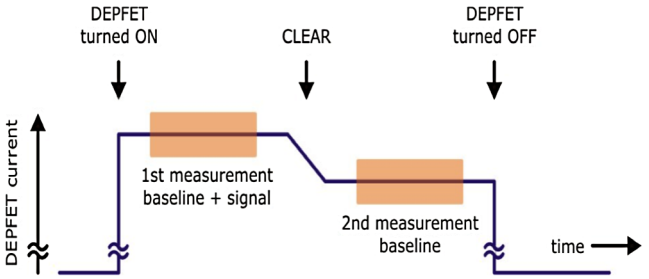

Fig. 5 Signal evaluation scheme for the readout of an active pixel sensor. After the integration time, the row is switched active by the use of an external gate and the total current is measured. Then, the charge in the internal gate is cleared completely and the current is measured again to determine the baseline offset. The difference of the two measurements gives the effective current that is proportional to the number of electrons collected in the internal gate and thus to the x-ray photon energy.

This scheme provides a high frame rate because of the simultaneous readout of all pixels of a row. The architecture of the DEPFET matrix and of the VERITAS-2 ASIC permits flexible readout modes, too, since arbitrary sub-areas of the matrix can be selected for readout. No charge transfer to readout nodes is necessary, as would be the case for a CCD. DEPFET APS are not affected by the predominant radiation damage effect of a CCD, the decrease of the charge transfer efficiency. This implies a significantly increased radiation hardness of the sensor.

3.2 *Front-End ASICs for Readout and Control*

Two different types of ASICs are needed to operate the DEPFET matrices: the readout ASIC and the switcher ASIC (see Fig. 6).

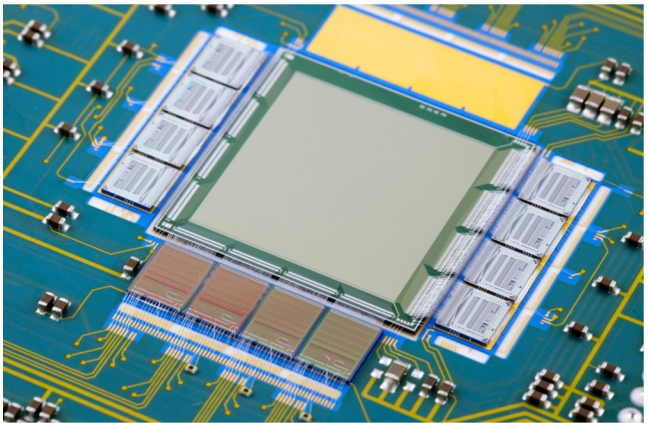

Fig. 6 Prototype DEPFET detector with 256×256 pixels developed in the course of the IXO project. The switcher ASICs are placed on the left- and right-hand side, whereas the readout ASICs (here of ASTEROID type) can be seen at the bottom.

The switcher ASIC is needed to switch a selected row to active by applying an appropriate voltage to the external gates of all pixels of the row. Furthermore, the charge clear pulses for the internal gates are applied by these ASICs. Two ASICs control an array of 64 DEPFET rows.

The readout ASIC of VERITAS-2[8] type will be tailored to the WFI DEPFETs. In addition to the typical source-follower readout, as used in the ASTEROID[9] ASICs for the MIXS flight detectors, it provides the possibility for drain-readout. For this purpose, a low-noise current-to-voltage converter is placed in front of the preamplifier. The main advantage of the drain-readout is that all the nodes of the DEPFET are at a fixed potential and the readout speed of the system is not limited by the resistor-capacitor (RC) time constant of the input of the readout chain. This capacitance comprises the input capacitance of the preamplifier and the parasitic capacitance associated with the DEPFET source line. Coupling the ASIC in the drain-readout mode with a DEPFET array enables a higher readout speed for the DEPFET matrix compared to the source follower mode. We aim for a readout time of 2.5 μs/row. The outputs of the analog channels of VERITAS-2 are serialized by a 64:1 multiplexer with a clocking speed up to 32 MHz and buffered by a fast fully differential output register. While the signals of a DEPFET matrix row are read out, the signals of the previous row are fed via the output buffer to the ADC. One VERITAS-2 ASIC processes 64 DEPFET channels.

The DEPFET and VERITAS-2 architecture allows window-mode readout of the pixel matrices. Selected sub-areas of the matrix can be addressed even with the option to read out different subareas with different speeds.

The switcher ASICs for the WFI will be based on the ASICs that have been developed for the MIXS detector onboard of the BepiColombo satellite. Regarding the VERITAS-2 ASIC, a first prototype version is currently under test. A detailed description is presented in Ref. 9.

3.3 *DEPFET for Large Areas and for Fast Readout*

The four large-area DEPFET matrices planned for the WFI essentially provide the field of view of 40 arc min. Each one comprises 448×640 pixels with a pixel size of 130×130 μm^2. The pixels can be slightly larger than 130×130 μm^2 for off-axis photon incidence because the point spread function

becomes worse with increasing off-axis angles. Thus a sufficient oversampling of the mirror's point spread function is still ensured. With the projected readout time per row of 2.5 μs (and assuming 640 rows and 448 channels per DEPFET sensor), we obtain a whole-DEPFET time resolution of 1.6 ms.

The unprecedented effective area of the Athena mirror system will provide very high photon rates for bright x-ray sources (e.g., ~100,000 count/s for the Crab pulsar). This necessitates very high frame rates and flexible readout modes which can be achieved by operating the 256×256 pixel central DEFET matrix in a window mode of e.g., 16 rows. Due to the excellent point spread function of 5 arc sec on-axis, a pixel size of 100×100 μm^2 (1.8×1.8 arcsec^2) was chosen for the central matrix. The matrix will be subdivided into two halves, each read out in parallel by four VERITAS-2 ASICs. With this concept, the WFI count rate capability will be optimized if the focal spot is located and maintained in a relatively precise position on this DEPFET sensor, which spreads the photons between the two readout halves. The feasibility of such a scheme and the impact on the pointing accuracy and stability shall be explored in the study phase. With the option to double the number of readout channels, two rows per half can be read out simultaneously. This allows the full chip to be read out in 160 μs or a 16-row window (corresponding to five times the on-axis PSF) in 10 μs. Since this option significantly increases the complexity of the detector and its power dissipation, therefore, a detailed trade-off is necessary during the technology development phase.

The more the readout time per row approaches the photon integration time, the higher is the probability for occurrence of so-called energy misfits. They are caused by analog signal processing errors from photons that hit the active row during the signal processing (see Fig. 5). The energy misfits can be prevented by an advanced version of DEPFETs, the gateable DEPFETs. They have an electronic shutter implemented into each active pixel, allowing suppression of x-ray photons that hit the pixel during the readout process. This improves the sensitivity and spectral response of the detector. The improvement by a gateable DEPFET compared to a nongateable DEPFET is demonstrated in Fig. 7.

In addition, advanced pixel layouts containing an intermediate storage region are in development. Charge generated during the readout is not lost but is collected in a region separated from the internal gate. This signal charge is read out in the next frame. The concept of gateable DEPFETs with an intermediate storage region minimizes dead time together with an increase of the sensitivity of the detector. Prototype devices have been designed, produced, and are currently being studied by testing and simulations. A detailed description of these devices is given in Ref. 10.

3.4 *WFI Detector Characteristics*

The expected performance of the WFI detectors is summarized in Table 1. The characteristics are based on the planned design, measurement results of existing detectors, and simulations. The energy spectrum of a prototype gateable DEPFET detector illuminated by an ^{55}Fe source is shown in Fig. 8 demonstrating the excellent energy resolution of the DEPFET, which is close to the theoretical limit given by the Fano-noise. This means the energy resolution is primarily limited by the statistical variation in the number of electrons generated in the silicon by the interacting x-ray photon. The spectroscopic performance capability of nongateable prototype DEPFET arrays has been verified in laboratory measurements. The goal is to maintain a spectral resolution with a full width at half maximum below 150 eV for a photon energy of 6 keV throughout the mission lifetime.

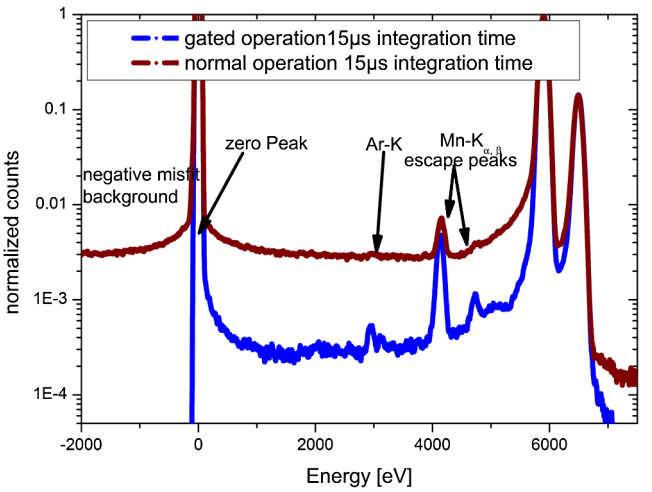

Fig. 7 Comparison of an ^{55}Fe spectrum measured with a standard DEPFET and a gateable DEPFET (i.e., with integrated electronic shutter) for a short integration time of 15 μs where the occurrence of energy misfits becomes relevant.[10] The gateable DEPFET shows approximately a factor of 10 less "background" because of the suppression of energy misfits caused by signal processing errors. Furthermore, the absence of absurd negative signal energies is demonstrated quite obviously.

Figure 9 shows an example for the resulting quantum efficiency of the WFI instrument that depends on the on-chip and external light-blocking filter (see Table 1). The filters are necessary to attenuate the visual and UV light intensities because the DEPFET is sensitive to these photon energies, too. In the energy band between 1 and 10 keV, the quantum efficiency is typically between 90% and 100%. The reason for this is the back-illumination of an unstructured and ultra-thin photon entrance window in combination with the full depletion of the 450-μm-thick DEPFET chip.

The effect of the quantum efficiency on the field of view averaged effective area is shown in Fig. 10. For energies below 1 keV, the effective area is significantly decreased by the WFI, whereas for energies above 1 keV, the effective area is determined solely by the mirror system. The effective area is at its maximum between 1 and 2 keV.

4 Detector Electronics

The detector electronics is part of the signal processing chain and provides the following main functionalities (see Fig. 11):

Time control of detector and electronics: A sequencer controls the VERITAS-2 and switcher ASICs for readout of the DEPFET sensors. This has to be synchronized with further signal processing comprising the ADCs and the frame processor. The sequencer, in turn, is controlled by the ICU.

Event processing: The frame processor receives as input the digitized signals of the detector pixels and has to conduct several corrections. This includes a pixel-wise offset correction, a row-wise common mode correction and filtering the photon signals out of signals caused by noise and particles. For the latter task, an energy window has to be defined and pattern analysis of the event needs to be performed. The extracted scientific data are sent to the ICU.

Table 1 Wide field imager (WFI) detector characteristics.

Parameter	Characteristics
Energy range	0.1 keV–15 keV
Field of view	40 arcmin in diameter
Angular resolution	mirror system: 5 arc sec (on-axis)
Fast DEPFET ×1	256 × 256 pixel subdivided in two halves
	100 μm × 100 μm pixel size (corr. to 1.8 × 1.8 arc sec^2)
	gateable DEPFET type with intermediate storage region
Large-area DEPFET ×4	448 × 640 pixel
	130 μm × 130 μm pixel size (corr. to 2.3 × 2.3 arc sec^2)
	nongateable DEPFET type
Quantum efficiency incl. external filter (70 nm Al on-chip; 40 nm Al + 320 nm PP ext. filter)	24% at 277 eV
	87% at 1 keV
	96% at 10 keV
Energy resolution	FWHM (6 keV) ≤ 150 eV
Time resolution	
Fast DEPFET full frame	320 μs (possibly 160 μs)
Fast DEPFET window mode (16 rows)	20 μs (possibly 10 μs)
Large DEPFET full frame	1.6 ms
Count rate capability (10 μs)	0.5 Crab: 88% throughput and 3% pile-up
	1 Crab: 79% throughput and 6% pile-up
Non-x-ray background (L2 orbit)	<5 × 10^{-3} cts cm^{-2} s^{-1} keV^{-1} (tbc)

Power conditioning: The detector electronics generates and supplies the necessary voltage signals to the camera head and components of the electronics according to commands sent by the ICU.

Houskeeping data: ADCs placed on the electronics boards measure the relevant analog voltage, current or temperature values of camera head and detector electronics and transfer the digital values to the ICU for analysis and control purposes.

5 Further Subsystems

Apart from the camera head and the detector electronics, the WFI instrument comprises further active subsystems:

Filter wheel subsystem (FW): The filter wheel controls the illumination of the detector and is mounted in the optical

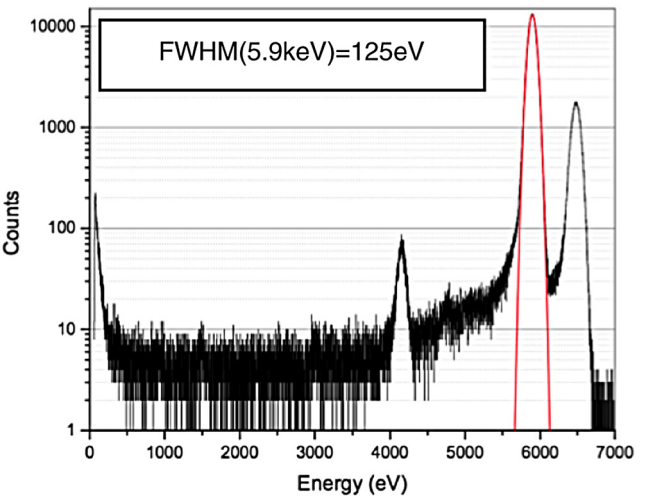

Fig. 8 Measurement of an ^{55}Fe source spectrum with a DEPFET sensor. A value of 125 eV was obtained for the full width at half maximum (FWHM) of the 5.9 keV line.

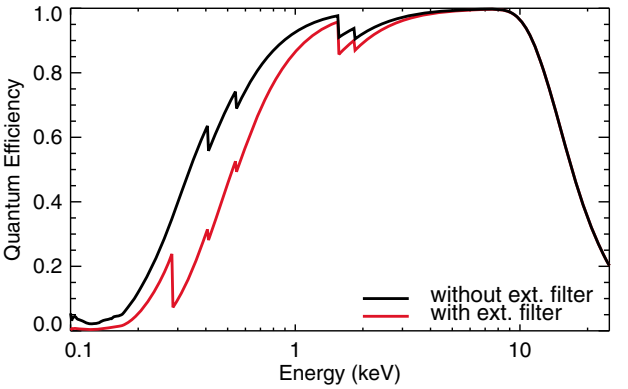

Fig. 9 Quantum efficiency of the projected WFI instrument. The black curve shows the values of the DEPFET sensor with on-chip light-blocking filter (70 nm aluminum), while the red curve shows the resulting quantum efficiency of the combination DEPFET with an additional external light-blocking filter (320 nm polypropylene and 40 nm aluminum).

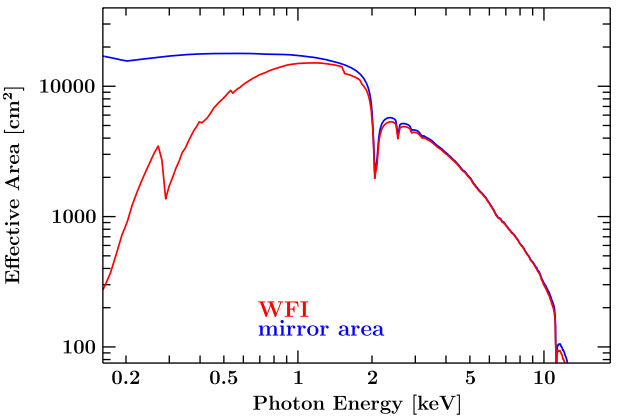

Fig. 10 Effective area provided by the Athena mirror system (blue curve) and resulting effective area for the WFI instrument (red curve) considering the quantum efficiency of the detector and the absorption by the external light-blocking filter. The presented values are averaged over the field of view, i.e., vignetting is taken into account.

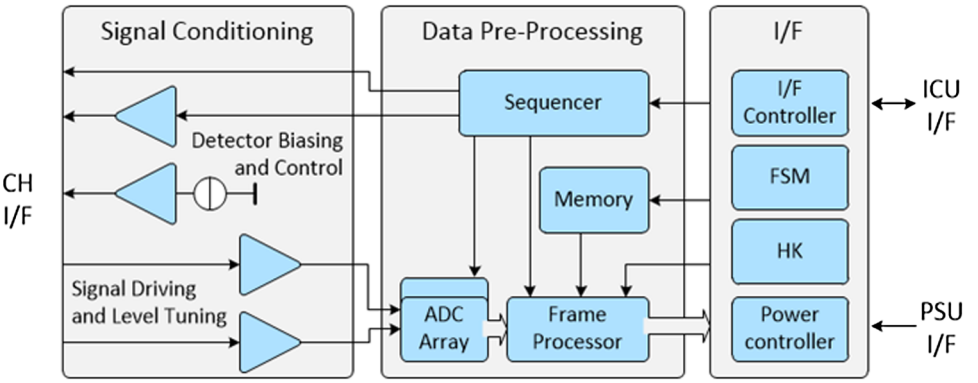

Fig. 11 The block diagram shows the detector electronics including the interfaces to the camera head and the ICU. Its main functions are power conditioning and data preprocessing.

path of the rays from the mirror system to the camera head. It offers four different options:

1. Illumination through a light-blocking filter. The filter should be arranged in a mosaic matched to the sensor array.
2. Open position for optimum evacuation of the camera and optional sensor illumination without external filter.
3. Illumination by on-board calibration source for recalibration of detector parameters in particular because of appearance of radiation damage effects. The source could be an ^{55}Fe source illuminating an Al-Ti target which results in the emission of the characteristic Mn-K_α, Mn-K_β lines and the Al and Ti fluorescence lines. Further details can be found in Ref. 6.
4. Closed position needed for shielding of the sensor against radiation (e.g., background studies) and protection of the camera on ground (e.g., during tests and launch).

The different options can be mounted on a filter wheel disk with a gear wheel driven by a stepper motor. Hall sensors can be used for position control. The motor controller can be accommodated in the ICU.

The light-blocking filter for the detector can be arranged as a mosaic of five single filters matched to the five DEPFET sensors. For mitigation of the risk that the ultra-thin filters are destroyed due to the acoustic noise caused by the rocket launch, a protection mechanism is likely necessary.

Power supply unit: The power supply unit (PSU) is the power interface to the satellite and supplies the electric power to the WFI camera after line filtering. It conditions the power to the appropriate voltage levels of the instrument. Furthermore, either latch current limiters or latch relays will be included in order to mitigate a power failure risk for the spacecraft and the other instruments. The PSU receives and executes high level commands for power on and off and provides the status signals for Housekeeping.

Instrument control unit: The ICU is the interface to the satellite (e.g., implemented as a space wire bus) with respect to the telemetry of scientific and Housekeeping data. It merges the data streams from the five detector units. The data need to be compressed before buffering in the mass memory of the satellite and transmission to ground. The ICU is also responsible for the decoding of telecommands sent from the ground station to the instrument. Additionally, it controls the instrument by internal telecommands sent to the detector electronics, the camera head, the power supply unit, the filter wheel, and the thermal control system.

Thermal system: A large-area radiator has to be thermally coupled via heat pipes to the focal plane detectors for cooling them to a sufficiently low operating temperature (less than or equal to −60°C). In addition, a constant operating temperature has to be maintained for optimum spectroscopic performance. This can be accomplished by the use of heaters attached to the thermomechanical structure of the focal plane. The thermal system is controlled by the ICU.

6 Schedule

After a study and technology development phase, which lasts until 2018, Athena will face mission adoption by ESA. The construction and test phases will follow, leading to the satellite launch in 2028. The operational lifetime is planned to be 5 years and the extended lifetime 10 years.

For the WFI instrument we assume the following tentative timeline:

- The announcement of opportunity for the Athena instruments is expected at the beginning of 2015. At this time, the WFI instrument consortium shall be established with the Max-Planck-Institut für Extraterrestrische Physik as the lead institute. After a first meeting in January 2014, frequent discussions with interested consortium members have been conducted and a protoconsortium evolves presently.
- During the technology development phase, a breadboard model is planned to be built and tested until 2018 in order to demonstrate technical readiness level 5/6.
- The development and test of the engineering model (EM) and structural and thermal model (STM) are projected until 2021.
- The development of the qualification model (QM) including qualification testing is planned between 2021 and 2024.
- The development of the flight model (FM) including the acceptance tests shall be finished by 2026.
- Launch of the Athena satellite is scheduled in 2028.

Acknowledgments

The authors are grateful to all colleagues who supported the Wide Field Imager instrument for Athena. This work was supported by DLR and the Dr. Johannes Heidenhain Stiftung.

References

1. K. Nandra et al., "The Hot and Energetic Universe," white paper submitted in response to ESA L2 call, arXiv:1306.2307 (2013).
2. R. Willingale et al., "The optical design of the Athena + mirror," supporting paper submitted in response to ESA L2 call, arXiv:1307.1709 (2013).
3. D. Barret et al., "The X-ray Integral Field Unit (X-IFU) for Athena+," supporting paper submitted in response to ESA L2 call, arXiv:1308.6784 (2013).
4. A. Rau et al., "The wide field imager (WFI) for Athena+," supporting paper submitted in response to ESA L2 call, arXiv:1308.6785 (2013).
5. N. Meidinger et al., "Development of the focal plane PNCCD camera system for the X-ray space telescope eROSITA," *Nucl. Instrum. Methods A* **624**, 321–329 (2010).
6. N. Meidinger et al., "Report on the eROSITA camera system," *Proc. SPIE* **9144**, 91441W (2014).
7. J. Treis et al., "MIXS on BepiColombo and its DEPFET based focal plane instrumentation," *Nucl. Instrum. Meth. A* **624**, 540–547 (2010).
8. M. Porro et al., "VERITAS 2.0 a multi channel readout ASIC suitable for the DEPFET arrays of the WFI for ATHENA," *Proc. SPIE* **9144**, 91445N (2014).
9. M. Porro et al., "ASTEROID: A 64 channel ASIC for source follower readout of DEPFET arrays for X-ray astronomy," *Nucl. Instrum. Methods A* **617**, 351–357 (2010).
10. A. Bähr et al., "Measurements on DEPFET APS improving time resolution, countrate capability, and throughput," *Proc. SPIE* **9144**, 914411 (2014).

Norbert Meidinger is senior staff instrument scientist at the Max-Planck-Institute for Extraterrestrial Physics (MPE), Germany. He received his MS and PhD in physics at the Technical University of Munich, Germany. His research area is the development of spectroscopic and imaging detectors for x-ray astronomy. He is the project manager of the WFI instrument on Athena.

Kirpal Nandra is director at the Max-Planck-Institute for Extraterrestrial Physics (MPE), Gemany. He is the PI of the WFI instrument on Athena.

Markus Plattner studied electronics engineering at the Technical University of Munich. From 2006 to 2010 he worked on his PhD thesis on opto-electronic technologies development for space applications. From 2010 to 2013 he worked at Kayser-Threde GmbH as system engineer and project manager. He led several space industry projects. In 2013 he joined the MPI for Extraterrestrial Physics as head of the Electronics Division. He is system engineer for the development of the WFI for ATHENA.

Arne Rau is a staff scientist at the Max-Planck Institute for Extraterrestrial Physics (MPE), Germany. He received his PhD in physics at the International Max-Planck Research School at the MPE and the Technical University of Munich. He is the WFI project scientist.

Biographies of the other authors are not available.